ISSN 0023-1584, Kinetics and Catalysis, 2017, Vol. 58, No. 5, pp. 593–600. © Pleiades Publishing, Ltd., 2017.
Original Russian Text © A.A. Vodyankin, I.P. Ushakov, Yu.A. Belik, O.V. Vodyankina, 2017, published in Kinetika i Kataliz, 2017, Vol. 58, No. 5, pp. 606–613.

Synthesis and Photocatalytic Properties of Materials Based on Bismuth Silicates[1]

A. A. Vodyankin*, I. P. Ushakov, Yu. A. Belik, and O. V. Vodyankina

National Research Tomsk State University, Tomsk, 634050 Russia

**e-mail: orzieorzie@gmail.com*

Received January 31, 2017

Abstract—The influence of the preparation technique of bismuth silicate-based catalysts on their formation, phase composition, absorption characteristics, and photocatalytic properties is investigated. Samples the with initial ratio of Bi : Si = 2 : 1 are prepared via the hydrothermal method with varied temperature conditions in the hydrothermal aging and calcination stages. The synthesized catalysts demonstrate photocatalytic activity in the decomposition of the methanol equilibrium vapor and visible light-induced decolorization of a methylene blue (MB) aqueous solution.

Keywords: bismuth silicates, hydrothermal synthesis, photocatalysis, methanol photodegradation, methylene blue decolorization

DOI: 10.1134/S0023158417050238

Researchers' attention is currently focused on materials with increased photocatalytic properties, a well-developed surface, and a high adsorption level. The most frequently used material for photocatalysis is titania due to it being highly active and due to its chemical stability, lack of toxicity, and relatively cheap price [1]. However, it also has disadvantages such as limited absorption spectra and the rapid recombination of charge carriers.

Lately interest in bismuth compounds (mainly silicates and titanates) has increased. Photocatalysts based on these materials are capable of working under visible light irradiation, which is beneficial in terms of saving energy. The photocatalytic characteristics of such systems strongly depend on phase composition, which is in turn defined by the preparation conditions and calcination temperature, amongst other factors [2].

In this study the influence of the conditions of the hydrothermal treatment (HTT) and subsequent calcination on the phase composition of bismuth silicate materials and their photocatalytic activity in model reactions is investigated. The first chosen model contaminant was a diluted equilibrium vapor of methanol due to its high degree of toxicity even in small amounts and frequent presence in industrial emissions. An additional testing reaction of the decolorization of a methylene blue (MB) aqueous solution under visible light was carried out.

EXPERIMENTAL

The bismuth silicate catalysts were prepared by the hydrothermal method. Sodium metasilicate $Na_2SiO_3 \cdot 5H_2O$ (chemically pure, Vekton, Russia) was used as a silicon source for series 1 and 2, while tetraethylorthosilicate $Si(OC_2H_5)_4$ (Sigma-Aldrich) was used for series 3 and 4. Bismuth nitrate $Bi(NO_3)_3 \cdot 5H_2O$ (chemically pure, Vekton, Russia) dissolved in ethylene glycol was used as a source of Bi in all four series of samples with the initial ratio of Bi : Si = 2 : 1.

Series 1 marked as BSN-1 (Bi–Si–Na) (samples BSN-150-1, BSN-160-1, BSN-170-1) was prepared by the method described in [3]. The calculated amounts of sodium metasilicate and bismuth nitrate were dissolved in distilled water and ethylene glycol, respectively, and then mixed together in a 100-mL Teflon autoclave to be subjected to HTT at 150, 160, and 170°C for 12 h. The obtained samples were dried at 50°C for 6 h and then calcined twice at 600°C with grinding in an agate mortar between calcinations.

Series 2 marked as BSN-2 (samples BSN-150-2, BSN-160-2, BSN-170-2) was prepared by a similar method; however, the calcination procedure was carried out only once at 500°C for 12 h.

Series 3 marked as BSO-1 (Bi–Si–O) (samples BSO-150-1, BSO-160-1, BSO-170-1) was prepared with the use of silicic acid sol. The calculated amount of tetraethylorthosilicate (TEOS) was mixed with distilled water in a molar ratio of TEOS : H_2O = 1 : 4, with the addition of concentrated nitric acid to achieve pH 2 with constant stirring for 15 min. The calculated amount of bismuth nitrate was dissolved in ethylene glycol. Both solutions were placed in a 100-mL Teflon autoclave and subjected to HTT at 150, 160, and 170°C for 12 h similarly to the other series. The obtained samples were dried at 50°C for 6 h and then calcined twice

[1] The article was translated by the authors.

at 600°C for 12 h with grinding in agate mortar between calcinations.

Series 4 marked as BSO-2 (samples BSO-150-2, BSO-160-2, BSO-170-2) was prepared via a technique similar to series 3 (BSO-1); however, the calcination procedure was carried out only once at 500°C for 12 h.

The surface area of the samples was evaluated via the low-temperature nitrogen adsorption method with the use of automatic adsorption TriStar II 3020 analyzer (Micromeritics, United States). The crystal structure of the synthesized materials was investigated by the X-ray diffraction method on a Shimadzu XRD 6000 diffractometer (Japan) with the use of CuK_α-radiation in the range of $2\theta = 20°–80°$ at a measurement speed of 2 deg/min. The optical characteristics of the prepared catalysts were studied with the use of a UV-spectrophotometer Cary-100 (Agilent, United States) in the diffuse reflectance mode (DR). Thermogravimetrical analysis (TGA) was carried out with the use of the Jupiter STA 449 F1 thermal analyzer (Netsch, Germany) in the temperature range of 25–900°C at a heating speed of 10 deg/min in an air atmosphere. The QMS 403 D Aëolos mass spectrometer (Netsch) was used to control the evolving decomposition products.

The photocatalytical activity of the samples was evaluated in two model reactions. The first experiment featured the decomposition of a methanol equilibrium vapor diluted with air, and thus imitating a low concentration air pollutant. The reaction was carried out in a vertical quartz reactor in the flow mode. Highly dispersed powders of the studied photocatalysts were immobilized on quartz chips (3–4 mm fraction) by the technique described in [4] with the use of an acetylacetone (chemically pure) suspension. To obtain the suspension, 0.3 mL of acetylacetone and 4.8 mL of distilled water was added to 0.750 g of a catalyst and the resulting mixture was ground in an agate mortar for 5 min. After that 19.2 mL of water was added to the mixture, which was then ground again for 5 min. The mixture was subjected to ultrasonic treatment for 10 min with the use of a YX 3560 (50 W) ultrasonic bath. A portion of the quartz carrier (40 g) was loaded into the suspension and left for 5 min. The operation was carried out twice. After that the extracted carrier was placed on an instrument glass and dried in a desiccator in room temperature for 48 h. Further thermal treatment of the samples was not executed. The content of the active component was 4 wt % for bismuth silicate catalysts, 2.6 wt % for α-Bi_2O_3, and 8 wt % for TiO_2.

The conversion of methanol was evaluated with the use of a Chromatec Crystal 5000.2 gas chromatograph (Chromatec, Russia). A methanol vapor was supplied by passing the air flow through a saturator with methanol (chemically pure) at a speed of 5 mL/min, which was then diluted with the second air flow to achieve the required concentration. The saturator was thermostated at 0°C with the use of an LOIP FT-311-25 cryostate. A mixture of ethylene glycol and water in the ratio of 1 : 1 was used as the heat carrier.

The second photocatalytical experiment featured the reaction of an MB photodegradation in an aqueous solution. The process was carried out in a quartz reactor in the static mode. A suspension of the catalyst in the studied solution (40 mL) was kept in darkness for 12 h to achieve adsorption equilibrium and then placed in a quartz reactor and irradiated for 3 h. Both stages of the experiment were carried out with constant stirring. The catalyst was separated from the studied solution via centrifugation for 2 min at a rotation speed of 15000 turns/min.

The irradiation source was an XHA-250 xenon lamp (250 W, 16 A, light flow 4800 lm.) with a PSL-C-250-10 power source (Razryad, Russia). The lamp's spectra were adjusted with the use of a YB-10 color filter ($\lambda = 400$ nm) during the MB photodegradation experiment.

TiO_2 Degussa P25 (Sigma-Aldrich) and α-Bi_2O_3 were used as reference samples in both the experiments. Bismuth oxide was obtained via calcining bismuth nitrate pentahydrate (analytical grade, Vekton) in a muffle furnace at 800°C for 2 h according to the equation

$$4Bi(NO_3)_3 \cdot 5H_2O \xrightarrow{800°C,\,2\,h} 2Bi_2O_3 + 12NO_2 + 3O_2 + 20H_2O.$$

RESULTS AND DISCUSSION

Phase Composition and Surface Area of Obtained Catalysts

The phase composition and surface characteristics of the obtained photocatalysts are presented in Table 1 and in Figs. 1 and 2. According to the obtained data, the main phase in all of the samples is sillenite $Bi_{12}SiO_{20}$. Small amounts of metastable bismuth metasilicate Bi_2SiO_5 and α-Bi_2O_3 are also observed. Also, the BSO-1 series obtained with the use of TEOS and calcined twice at 600°C contains a high proportion of eulytite $Bi_4Si_3O_{12}$.

According to the literature [5], sillenite possesses a body-centered cubic structure similar to metastable γ-Bi_2O_3 (natural sillenite), which is stabilized in the presence of metal oxides in the ratio of M : Bi = 1 : 12. Sillenite crystal consists of SiO_4 tetrahedra and distorted $BiO_5\square$ octahedra ("□" indicates a vacancy). Bismuth orthosilicate $Bi_4Si_3O_{12}$ belongs to the eulytite family, possessing a cubic structure with 4 formula units in the grid, where each Bi ion is coordinated by a distorted octahedron of oxygen atoms belonging to the

Table 1. Surface area and phase composition of prepared bismuth silicates and reference samples (α-Bi_2O_3 and TiO_2)

Sample		S, m^2/g	Phase composition, vol %			
			$Bi_{12}SiO_{20}$	$Bi_4Si_3O_{12}$	Bi_2SiO_5	α-Bi_2O_3
Series 1 (BSN-1)	BSN-150-1	2	90	–	3	7
	BSN-160-1	<1	87	–	3	10
	BSN-170-1	1	85	–	13	2
Series 2 (BSN-2)	BSN-150-2	1	91	–	6	3
	BSN-160-2	<1	95	–	3	2
	BSN-170-2	<1	94	–	4	2
Series 3 (BSO-1)	BSO-150-1	<1	45	44	11	–
	BSO-160-1	11	54	35	11	–
	BSO-170-1	12	50	43	7	–
Series 4 (BSO-2)	BSO-150-2	1	57	–	24	19
	BSO-160-2	4	45	–	24	31
	BSO-170-2	<1	49	–	42	9
Reference samples	α-Bi_2O_3	<1	–	–	–	100
	TiO_2	55	(70% anatase, 30% rutile)			

neighbouring silicate ions, while the Bi cations are placed on the C_3 axis of symmetry and the SiO_4 tetrahedra are stationed in the S_4 position [6].

Bismuth metasilicate Bi_2SiO_5 possesses an orthorhombical structure and belongs to the Aurivillius phase family [7], where $Bi_2O_2^{2+}$ layers consisting of square-based pyramids with oxygen atoms in the base are alternated with perovskite-like layers $A_mB_{m-1}O_{3m+1}^{2-}$, where m is the number of octahedra perpendicular to the Bi_2O_2 layers. For $m = 1$ perovskite-like layers are composed of MO_4^{2-} structural units and are replaced with SiO_3^{2-} pyroxene layers in the case of silicon having lesser valence.

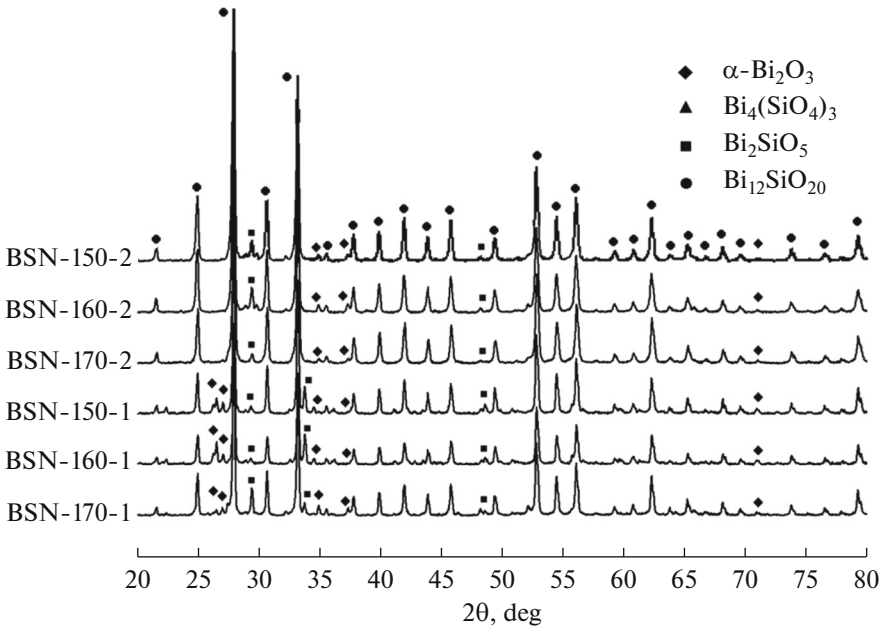

Fig. 1. Phase composition of synthesized samples of series 1 (BSN-1) and 2 (BSN-2) prepared with use of sodium metasilicate.

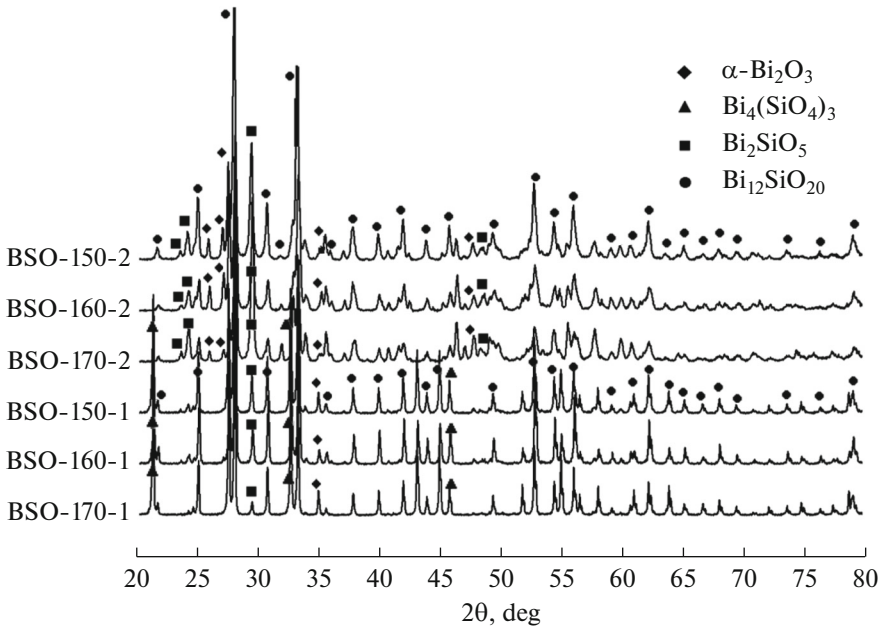

Fig. 2. Phase composition of synthesized samples of series 3 (BSO-1) and 4 (BSO-2) prepared with use of tetraethylorthosilicate.

The BSN-1 and BSN-2 series obtained with the use of Na_2SiO_3 as the silicon source are characterized with the biggest amount of the sillenite phase. With the variation of the thermal treatment conditions the phase composition of these series barely changes, apart from the BSN-160-1 and BSN-170-1 samples possessing a higher amount of impurity phases, to 10–13 rel. % of α-Bi_2O_3 and Bi_2SiO_5.

The proportion of impurity phases in the BSO-1 and BSO-2 series obtained with the use of TEOS is noticeably higher. Besides sillenite, for the BSO-1 series, the eulytite $Bi_4Si_3O_{12}$ phase was also detected in a comparable amount, while for the BSO-2 series, it was completely absent in the presence of α-Bi_2O_3 and an increased amount of bismuth metasilicate Bi_2SiO_5. The calcination conditions notably affect the phase composition for this series, which is connected with the metastability of the Bi_2SiO_5 phase [8], which is transformed to $Bi_4Si_3O_{12}$ under an increased temperature, in addition to the already formed eulytite.

To sum up, the BSN-1 and BSN-2 series possess a similar well-crystallized structure with sillenite present as the main phase. The use of TEOS as the source of silicon (BSO-1 and BSO-2) leads to a change in the phase composition of the samples. The phase composition of the obtained materials is mainly influeced by the time and temperature of calcination, while the influence of the HTT temperature is notably lower.

Study of the Obtained Materials by Diffuse Reflectance Spectroscopy

The optical properties of the prepared materials and reference samples in the UV and visible range are shown in Fig. 3. According to the obtained data, all the synthesized materials demonstrate absorption in the visible range in addition to increased adsorption in the area of 330 nm characteristic for the Bi–O–Bi bonds [9].

Figure 3a shows a comparison of the absorption spectra for the BSN-1 and BSO-1 series calcined twice at 600°C but prepared with different Si precursors (sodium metasilicate and TEOS, respectively). As shown, the BSN-1 series demonstrate stronger absorption in the UV and visible range. It should be noted that the absorption characteristics of the BSO-150-1 and BSO-160-1 barely differ. The absorption curve of the BSO-170-1 sample demonstrates notably lower absorption in the area of 450 nm than the other photocatalysts from this series, which may be attributed to the different impurity phase composition in the layered structure of the sample.

A comparison of the absorption spectra for the BSO-1 and BSO-2 series prepared with the use of TEOS with varied temperature and treatment time is presented in Fig. 3b. The curves of the BSO-2 series behave differently and notably differ from each other; this is related to the difference in their phase composition. Sample BSO-170-2 containing the least amount of the bismuth oxide impurity and the largest percentage of metastable Bi_2SiO_5 demonstrates the highest absorption in the area of 480 nm. We can conclude

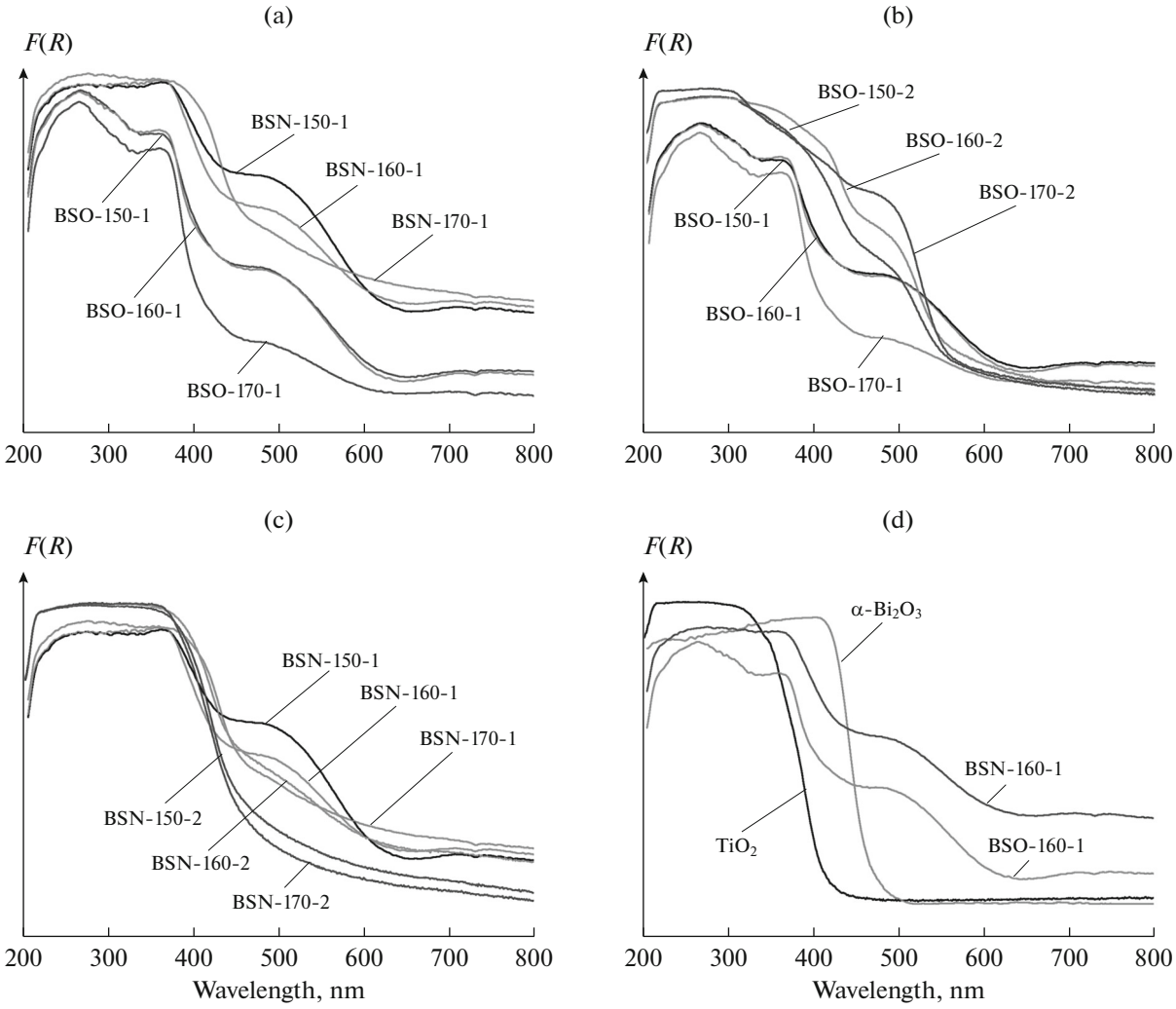

Fig. 3. Study of absorption spectra of synthesized materials. (a) Influence of precursor nature in BSN-1 and BSO-1 sample series. Influence on thermal treatment conditions for BSO-1 and BSO-2 (b) and BSN-1 and BSN-2 (c). (d) Comparison of absorption spectra of synthesized materials (BSN-160-1 and BSO-160-1), as well as reference samples (α-Bi_2O_3 and TiO_2).

that calcination at higher temperature lowers the absorption of the UV and visible radiation for the samples obtained with the use of TEOS. This is correlated with the difference in their phase composition where, for the BSO-1 metastable phase, Bi_2SiO_5 is able to transform to a more stable $Bi_3Si_4O_{12}$ phase having less absorption in the visible range.

Figure 3c illustrates a comparison of the absorption spectra for the BSN-1 and BSN-2 series; both were prepared with the use of sodium metasilicate but calcined twice at 600°C and once at 500°C, respectively. The absorption of the UV and visible irradiation for BSN-1 series is notably lower than for the BSN-2 calcined at a lower temperature.

Figure 4d shows the absorption characteristics of the prepared BSN-160-1 and BSO-160-1 silicates, as well as the reference samples, α-Bi_2O_3 and TiO_2. All bismuth silicates studied in this work demonstrate higher absorption in the visible range than the reference samples, which influences their activity, as it will be presented in the study of their photocatalytical properties.

Thermogravimetrical Study Results

The TGA (DSC) method was used to investigate the patterns for the formation of the structure of the obtained bismuth silicates. The TG-DSC curves for the BSN-160-1 and BSO-160-1 samples dried at 50°C for 6h are shown in Fig. 4.

The studied samples lose mass in the range of 25 to 100°C on the TG curves, which is attributed to the water desorption, according to the mass spectrometric analysis, while the exothermal peaks in the area of 260–300°C are connected with the combustion of organic impurities according to the CO_2 evolution

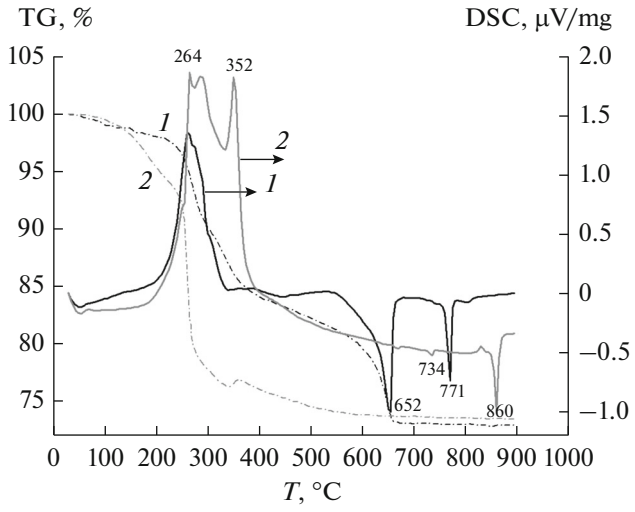

Fig. 4. TG–DSC curves for samples BSN-160-1 (*1*) and BSO-160-1 (*2*) after HTT and drying at 50°C for 6h.

curve. According to the published data [10], the area of 230–240°C can also be attributed to the decomposition of $Bi(OH)_3$ with the formation of BiOOH and the further decomposition to amorphous bismuth oxide at 320°C. The results of the mass spectrometrical analysis of the evolving gases (not shown in the figures) showed that the evolution of nitrogen oxides (NO and NO_2) in the area of 250–300°C also takes place, indicating the decomposition of unreacted nitrates. On the TG curve of the BSO-160-1 sample prepared with the use of TEOS, an additional exothermal peak is detected at 352°C, which is attributed to the combustion of organic impurities (evolution of CO_2).

An endothermic peak characteristic for the decomposition of nitrogen oxides is detected in the medium temperature range (650–670°C) on the TG curve for the BSN-160-1 sample. During the decomposition process of the precursor for BSO-160-1 this peak is less expressed and is not accompanied with a notable evolution of nitrogen oxides, which indicates a different composition of the precipitates forming after the HTT.

The high-temperature endothermic peaks at 770 and 800–810°C (BSN-160-1), as well as 730 and 860°C (BSO-160-1), not connected with the decrease of the mass, can be attributed to the phase transitions in these systems. According to [10], the metastable phase of Bi_2SiO_5 is able to react with amorphous silica at temperatures above 715°C with the formation of eulytite $Bi_3Si_4O_{12}$. This closely agrees with the XRD data for the BSO-1 series (Fig. 2, Table 1) and explains the absence of the $Bi_3Si_4O_{12}$ phase in the BSO-2 series calcined at a lower temperature. In general we can conclude that the main phase composition of the prepared samples is formed in the low temperature area (200–300°C) and is defined primarily by the HTT conditions, because the main phase in all the synthesized silicates is sillenite $Bi_{12}SiO_{20}$, which is present even in the BSN-2 and BSO-2 series calcined at a lower temperature (Table 1).

Photocatalytical Properties of the Prepared Materials Based on Bismuth Silicates

Table 2 presents the results of the photocatalytical study of the synthesized materials and reference samples: TiO_2 and α-Bi_2O_3. According to the obtained data, the BSN-1 series prepared with the use of sodium metasilicate and calcined twice at 600°C is the most active in both the catalytical experiments, with the BSN-160-1 sample showing the highest activity of all the synthesized silicates.

Despite the fact that the photocatalytical activity tends to grow with the HTT temperature increasing from 150°C (BSN-150-1) to 160°C (BSN-160-1), the further increase of the temperature to 170°C (BSN-170-1) leads to a significant decrease in the conversion of both methanol and MB in the discussed reactions. This is connected with the difference in the phase composition formed in the nucleation stage and confirms the influence of the HTT temperature on the phase formation process. Moreover, it is important to note that the BSN-2 series also obtained with the use of sodium metasilicate but calcined once at 500°C demonstrates notable photocatalytical activity (as well as BSN-1), which may be connected with the prevalence of the sillenite phase (as shown by the authors of [11] in studying $Bi_{12}SiO_{20}$ nanofibers prepared with the electric spindle method). The conversion values for the BSN-2 series are more or less comparable with the results of the BSN-1 study save for the BSN-150-2 sample showing the lowest activity. Finally, it was determined that the less active catalysts in the second experiment from the BSN-1 and BSN-2 series prepared with the use of sodium metasilicate are characterized with the largest amount of the metastable Bi_2SiO_5 phase. Thus, we can conclude that the temperature of the HTT for the samples prepared with the use of sodium metasilicate plays a key role in the formation of photoactive catalysts because their crystal structure is notably more thermally stable than the structure of samples of the BSO-1 and BSO-2 series.

A different situation is observed for samples of the BSO-1 series prepared with the use of TEOS and calcined twice at 600°C, which practically do not show any activity in either of the catalytic experiments. This can be connected with the significant amount of eulytite $Bi_4Si_3O_{12}$ in the phase composition of the samples. Characteristically, the samples of the BSO-2 series calcined at a lower temperature and not possessing this phase demonstrate noticeably higher activity in both decomposing methanol and MB having an increased amount of α-Bi_2O_3 and Bi_2SiO_5 in their phase composition. It is possible that the presence of α-Bi_2O_3 has a certain effect due to its ability to participate in the

Table 2. Photocatalytical activity of prepared bismuth silicate catalysts

Catalyst		T_{HTT}, °C	$T_{calcination}$, °C	Methanol conversion, %	MB conversion, %
Series 1 (BSN-1)	BSN-150-1	150	600 (stage 1) 600 (stage 2)	22.4	36
	BSN-160-1	160	600 (stage 1) 600 (stage 2)	25.9	43
	BSN-170-1	170	600 (stage 1) 600 (stage 2)	15.0	19
Series 2 (BSN-2)	BSN-150-2	150	500	19.3	17
	BSN-160-2	160	500	19.7	29
	BSN-170-2	170	500	14.9	20
Series 3 (BSO-1)	BSO-150-1	150	600 (stage 1) 600 (stage 2)	1.8	0
	BSO-160-1	160	600 (stage 1) 600 (stage 2)	2.2	0
	BSO-170-1	170	600 (stage 1) 600 (stage 2)	2.0	0
Series 4 (BSO-2)	BSO-150-2	150	500	10.3	9
	BSO-160-2	160	500	9.8	10
	BSO-170-2	170	500	11.4	11
Reference samples	α-Bi_2O_3	–	–	11.2	8
	TiO_2	–	–	6.4	0

photocatalytical reactions initiated by visible light (as shown in [12], while studying the Bi_2O_3 wires obtained by the hydrothermal method), as well as due to the comparable conversion values of MB in the second experiment for BSO-2 and individual α-Bi_2O_3. In general, the calcination conditions for samples of the BSO-1 and BSO-2 series significantly influence the crystal structure of the obtained systems and their photocatalytical activity. It should also be noted that all the studied bismuth silicates (apart from the BSO-1 series) demonstrate increased photocatalytical activity compared with the TiO_2 reference sample, which did not show any activity in the experiment with MB carried out in the liquid phase under visible light irradiation.

CONCLUSIONS

The temperature of the HTT and the nature of the silicon precursor has the strongest influences on the phase composition and optical properties of the obtained bismuth silicate materials, as well as on their photocatalytical activity. The calcination conditions are also important for the crystal structure of such systems. The main phase in all the studied materials is sillenite ($Bi_{12}SiO_{20}$), an increased amount of which determines the high level of photocatalytical activity of the samples of the BSN-1 and BSN-2 series obtained with the use of sodium metasilicate. The bismuth metasilicate Bi_2SiO_5 phase is thermally unstable and transforms into the eulytite $Bi_4Si_3O_{12}$ phase with a change in stoichiometry. However, the BSO-2 samples containing an increased amount of the unstable phase, as well as α-Bi_2O_3, demonstrate a notably higher activity level than the materials having an increased amount of eulytite (BSO-1), especially in the decomposition of MB in an aqueous solution under the visible light irradiation.

ACKNOWLEDGMENTS

The work was carried out as part of a government task of the Russian Ministry of Education and Science, project no. 4.4590.2017/6.7.

REFERENCES

1. Carp, O. Huisman, C.L., and Reller, A., *Prog. Solid State Chem.,* 2004, vol. 32, p. 33.

2. Batool, S.S., Hassan, S., Imran, Z., Rasool, K., Ahmad, M., and Rafiq, M.A., *Int. J. Environ. Sci. Technol.,* 2016, vol. 13, p. 1497.
3. Duan, J., Liu, Y., Pan, X., Zhang, Y., Yu, J., Nakajim, K., and Taniguchi, H., *Catal. Commun.,* 2013, vol. 39, p. 65.
4. Zvereva, I., Kalinkina, L., Rodionov, I., Sankovich, A., Kolesnik, I., and Gudilin, E., *Glass Physi. Chem.,* 2012, vol. 38, p. 504.
5. Wiehl, L., Friedrich, A., Haussuhl, E., Morgenroth, W., Grzechnik, A., Friese, K., Winkler, B., Refson, K., and Milman, V., *J. Phys.: Condens. Matter,* 2010, vol. 22, p. 5401.
6. Ravindran, T., Arora, A., and Gopalakrishnan, R., *J. Phys.: Condens. Matter,* 2002, vol. 14, p. 6579.
7. Georges, S., Goutenoire, F., and Lacorre, P., *J. Solid State Chem.,* 2006, vol. 179, p. 4020.
8. Guo, H., Wang, X., and Gao, D., *Mater. Lett.,* 2012, vol. 67, p. 280.
9. Police, A., Basavaraju, S., Valluri, D., and Machiraju, S., *J. Mater. Sci. Technol.,* 2013, vol. 29, p. 639.
10. Bai, Z., Ba, X., Jia, R., Liu, B., Xiao, Z., and Zhang, X., *Front. Chem. China,* 2007, vol. 2, no. 2, p. 131.
11. Dongfang, H., Xianluo, H., Yanwei, W., Bin, S., Pei, H., Xiaoqin, X., Yun, Q., and Yunhui, H., *Phys. Chem. Chem. Phys.,* 2013, vol. 15, p. 20698.
12. Jinli, H., Hongmei, L., Caijin, H., Min, L., and Xiaoqing, Q., *Appl. Catal., B,* 2013, vols. 142–143, p. 598.